10 Jan 2018

Nano-Graphene Oxide and Vitamin D Delivery

Reza Mahdavi

Mehran Solati-Hashjin

Meisam Omidi

Arash Khojasteh

et. al. For a complete list of authors, see https://scholarsmine.mst.edu/mec_aereng_facwork/5055

Recommended Citation

R. Mahdavi et al., "Nano-Graphene Oxide and Vitamin D Delivery," *AIP Conference Proceedings*, vol. 1920, article no. 20008, American Institute of Physics, Jan 2018.
The definitive version is available at https://doi.org/10.1063/1.5018940

RESEARCH ARTICLE | JANUARY 10 2018

Nano-graphene oxide and vitamin D delivery

Reza Mahdavi; Mehran Solati-Hashjin; Meisam Omidi; ... et. al

AIP Conference Proceedings 1920, 020008 (2018)
https://doi.org/10.1063/1.5018940

Nano-graphene Oxide and Vitamin D Delivery

Reza Mahdavi[1, 2, b)], Mehran Solati-Hashjin[1, a)], Meisam Omidi[2, c)], Arash Khojasteh[3, d)], Fateme Fayyazbakhsh[1, e)]

[1] *Faculty of Biomedical Engineering, Amirkabir University of Technology (Tehran Polytechnic), 424 Hafez Ave, Tehran, Iran.*
[2] *Department of Tissue Engineering and Regenerative Medicine, School of Advanced Technologies in Medicine, Shahid Beheshti University of Medical Sciences, Taleghani University Hospital, Tehran, Iran.*
[3] *Department of Oral and Maxillofacial Surgery, School of Advanced Technologies in Medicine, Shahid Beheshti University of Medical Sciences, Taleghani University Hospital, Tehran, Iran.*

[a)] Corresponding author: Mehran.solati@gmail.com
[b)] Reza.mahdavi1371@gmail.com
[c)] Maysam.omidi@gmail.com
[d)] arashkhojasteh@yahoo.com
[e)] f.fba.te@gmail.com

Abstract. One of the most interesting and recent insights into biomimetic scaffold nano-biomaterial is smart scaffolding with targeted drug delivery ability. In recent decades, the use of graphene-based materials, such as nano-graphene oxide (nGO), as a drug carrier with amphiphilic properties, has attracted considerable attention of scientists and researchers in this field. In addition, one of the important global problems is increased vitamin D deficiency, particularly in pregnant and postmenopausal women. Therefore, in this work, by considering hydrophobic properties of vitamin D, we attempted to examine its loading and release both in the presence of surfactant and surfactant-free nGO-aqueous solution. At first, nGO powder was synthesized by the modified Hummer's method. After the preparation of vitamin D and Tween 80 (TW) solution, they were added to nGO aqueous solution. Simultaneously, the next vitamin D and nGO aqueous solution was prepared in a surfactant-free mode. In order to evaluate the loading content, both solutions were centrifuged, and their supernatant was analyzed by UV-Visible spectroscopy. Additionally, FTIR spectroscopy was employed to determine the TW 80 effects on vitamin D and nGO. The results have shown that vitamin D loading in surfactant-free solution was approximately 0% while in the presence of TW 80 it was 75.37% ± 4.12. Therefore, the combination of vitamin D, TW 80, and nGO can be a suitable candidate for carrying hydrophobic drugs in smart scaffolding, especially in bone tissue engineering.

INTRODUCTION

Vitamin D_3 (VD) as a fat-soluble nutrient has vital effects on human health. It already showed that VD has an ability to inhibit cancer cell proliferation, especially in breast, colon, and prostate tumor [1-4]. There are two different forms of VD in the body, Endogenous and Exogenous. Skin UV exposure results in the endogenous VD synthesizing while the exogenous form has dietary sources, particularly dairy products and fish oil [5, 6]. Although there are many different reports on the benefits of VD administration, it has been reported that excessive amount of VD causes kidney stone formation followed by increased bone resorption [7, 8]. In this regard, a number of various delivery systems have previously been utilized to optimize VD bioavailability and its related functions, including: titanium implants VD-coated [9], nano-emulsion [10], nano-encapsulation [11], lipid microparticle [12, 13], and lipoprotein core-shell complex [14].

Nano-particle-based drug delivery is one of the most common strategies in delivery systems that have a further advantage in comparison to microparticle carriers. A wide range of drugs such as hydrophobic drugs, biomolecules, DNA, etc. can be delivered in this manner because of their versatility and encapsulation potential [15]. In recent years,

6th International Biennial Conference on Ultrafine Grained and Nanostructured Materials
AIP Conf. Proc. 1920, 020008-1–020008-7; https://doi.org/10.1063/1.5018940
Published by AIP Publishing. 978-0-7354-1612-3/$30.00

nano-graphene oxide (nGO) has been extensively explored as a biomaterial for bioapplications such as imaging, cancer treatment, drug delivery, and tissue engineering [16-18]. Besides the different methods in lipophilic drug-delivery systems, nano-carriers such as nGO have been introduced as the most convenient means in this approach [19]. Its large surface area, amphiphilicity, cost effective synthesizing process, two-dimensional planer structure, outstanding biocompatibility and conceivably of simple functionalization provides some excellent opportunities for drug delivery applications [20-22]. In this context, drug molecules bind to the solid surface of nGO planes through π-π stacking interactions and its different functional groups, i.e. epoxide, carboxylic, and hydroxyl provide more stability in drug-nGO conjugation [23].

By considering the aqueous environment of the body, it seems that no single strategy is appropriate for lipophilic drug delivery. Instead, surfactant-based delivery systems in combination with nano-graphene oxide can be the most efficient colloidal delivery system in every specific lipophilic component [24]. Polysorbate 80 also known as tween® 80 has been extensively used as an emulsifier in foods, cosmetics, medicine, and laboratory research [25]. Recently, owing to its biocompatibility, it has been employed as a coating agent to cross drug particles over the blood-brain barrier (BBB) [26-28]. In this study, the role of nGO as a VD carrier was investigated in the presence of surfactant and surfactant-free media.

EXPERIMENTAL

Materials and Equipment

All chemicals used were reagent grade and included the following: graphite nano-flake (Merck), hydrogen peroxide (H_2O_2) (Merck), sulfuric acid (H_2SO_4 98%) (Merck), potassium permanganate ($KMnO_4$) (Merck), hydrochloric acid (HCl) (Merck), and sodium nitrate ($NaNO_3$) (Merck). Polysorbate 80 (TW® 80) and vitamin D were kindly gifted by Dr. Meisam Omidi and Osvah Pharmaceutical Company, respectively. The UV absorption spectra of VD and nGO compound were collected by using a Camspec UV-Visible spectrophotometer over the wavelength range from 190nm to 900nm. The chemical structure and functional groups of synthesized material and VD were studied by Fourier transform infrared (FTIR) of Thermo Nicolet Spectrometer (USA). The crystallographic structure of synthesized nGO powder was examined by an EQuinox 3000 (Inel, French) diffractometer with 40kV voltage and 30mA current setting, using Cu-Kα radiation (1.54187°A). To record XRD patterns, all the samples were scanned in the range of $5 \leq 2\theta \leq 110$.

Synthesis of nGO and Loading Procedure

nGO was prepared according to the modified Hummer's method [29]. Briefly, native graphite powder (1 g) was added to concentrated H_2SO_4 (120 ml). In order to cool the reaction environment, the whole setup was placed in an ice bath and $NaNO_3$ (500 mg) was added slowly. $KMnO_4$ (6 g) was added gradually to the mixture with constant stirring and the temperature was kept at 35°C for 48h. By the end of the time, the brownish green mixture became too viscose to stir. After that 400 ml double distilled water (DDW) was added to terminate the reaction while keeping the temperature below 70°C for one hour. Subsequently, by adding 30% H_2O_2 (10 ml) the color of the mixture changed to brilliant yellow, as described by Imani et al. [30]. Then, the mixture was stored for 2 days at room temperature to precipitate. The supernatant was removed, and the precipitate was washed and centrifuged with 0.5M HCl (300 ml). Finally, to remove acid residue, nGO sheets were rinsed with DDW until the pH of the solution neutralized and dried in the oven at 50°C for 24h to achieve nGO powder.

To obtain nano-graphene oxide and prepare stock solution, 1 g nGO was cracked in 95.5 ml DDW by an ultrasonic probe for 15 min. After that, 500 µl TW 80 was added to the solution as a surfactant and mixed for 24h until the dissolution of the formed bubbles. In this work, Taguchi's design of experiment methodology has been used for designing the experiment and optimizing drug:carrier mass ratio. Before testing any experiment, to determine loading amount, the standard curve with r^2=0.9744 was plotted using the results of the serial dilution standards at 256 nm (Fig 2c).

The Taguchi method organizes affecting parameters and their levels at which they could be varied. In this work, TW amount as a loading media and VD: GO ratios were considered as the factors and their variations were set as their levels according to Table 1. Therefore, 9 experiments have been set to evaluate GO loading capacity. To quantify VD loading efficiency, each sample was prepared according to Table 1 and was shaken for 1h in dark conditions. All the

solution was centrifuged and 100 µl of the supernatants was diluted in 0.5% TW solution (5 ml). The free VD amount (W_{free} VD) in the solutions were determined by UV-Visible spectrometer, and then the VD-loading efficiency was measured by equation [31]:

$$\% \text{ VD loading efficiency} = (W_{feed}\,\text{VD} - W_{free}\,\text{VD}) \times 100 / W_{feed}\,\text{VD}$$

TABLE 1. Prepared samples according to Taguchi method

#	TW (ml)	VD:GO	RPD (%)	#	TW (ml)	VD:GO	RPD (%)	#	TW (ml)	VD:GO	RPD (%)
1	50	1:1	27.37	**4**	50	1:5	55.57	**7**	50	1:10	63.8756
2	35	1:1	26.61	**5**	35	1:5	82.22	**8**	35	1:10	58.3867
3	20	1:1	19.8911	**6**	20	1:5	108.036	**9**	20	1:10	68.12

*Relation percent of deference (loading value per maximum)

RESULTS AND DISCUSSION

Phase analysis

Fig. 1d shows the XRD pattern of synthesized nGO and confirms the formation of GO nano-sheets. In this case, a typical diffraction peak at about 2θ=11.5 corresponds to the (002) plane with d-spacing 7.69586 Å and indicates that the oxidation process has been done properly. As it can be seen, there is no extra specific diffraction peak, which shows the formation of functional groups (i.e. epoxy, hydroxyl and carboxyl) between the graphite sheets. The presence of the functional group can make facile exfoliation via sonication, which is followed by increased interlayer spacing [32]. Therefore, these findings confirm nGO formation.

Drug Loading Evaluation

As it was previously mentioned, nGO has a large surface area. Thus, it is supposed to show the excellent loading behavior. The targeting samples were prepared as described in section 2.2. After the preparation of samples, a UV-Visible spectrophotometer was used to evaluate the loading percentage. We also prepared water/VD solution as a negative control sample. It was found that VD formed a second phase in water due to the hydrophobicity of VD. The loading efficiency was determined by a UV-Visible spectrophotometer. The VD conjugated nGO in surfactant-free media has nearly the same loading efficiency of water/VD (approximately 0%), containing the same concentration of VD, apart from the fact that the formation of the second phase (drug phase) was a delayed process. While when the TW 80 was added to the aqueous solution of nGO and VD, the stability of the solution extremely increased without any phase separation.

To analyze the results, the Taguchi analysis method has been used. Accordingly, in Fig. 1 which shows RPD plotting, “A” is referred to VD:GO ratio in 3 different levels of TW solution (50, 35, and 20 ml) and “B” represents each TW solution in different VD:GO ratios (1:1, 1:5, and 1:10). As it can be seen in Fig. 1a, the A factor in the first level (1:1) which shows the average of loading percentage of three different TW solutions (50, 35, and 20ml), has the lowest value. This is while according to Fig. 1b, it is in the maximum value. This means that the same proportion of GO to VD mass ratio has the highest level of loading percentage (75.37% ± 4.12).

In contrast, in the second level of A diagram, the average loading percentage in three different TW solutions is in the highest and lowest value in Fig. 1a and Fig. 1b, respectively. This means that the 1:5 VD:GO ratio cannot be considered as a suitable proportion to drug loading. Unlikely, in the third level of A diagram in Fig. 1a which represents the lowest VD:GO ratio (1:10), moderate drug loading is shown. This means that when there is a need for the most efficient and mildest VD loading percentage, it can be chosen as the best ratio. In this case, the loading efficiency was reached at 36.87% ± 4.87 (n=3) according to the standard curve (Fig 2c).

The second diagram at the right side of Fig. 1 (B) confirms all the former results. In these two plots, "B" represents the amount of TW solution against three different VD:GO ratios. Each point is an average of three different VD:GO ratios. As it can be seen in Fig. 1a part B, the first point shows the average of three VD:GO ratios in the 50ml of TW solution. In this point, the loading percentage is at the lowest value. In contrast, in the mean of signal-to-noise ratio diagram (Fig. 1b), this point is in the highest level, the results of which confirm the maximum loading percentage in the 1:1 VD:GO ratio. As it has been previously mentioned, there are no significant differences in Fig. 1a and Fig. 1b for the second point of B diagram (35ml TW solution in three different VD:GO ratios). Therefore, it confirms the last observed result that it cannot be considered as a suitable drug loading ratio and media solution. Instead, the third point of B diagram in both figures shows that the diminished level of the drug can encourage GO sheets to increased physical interaction with VD molecules.

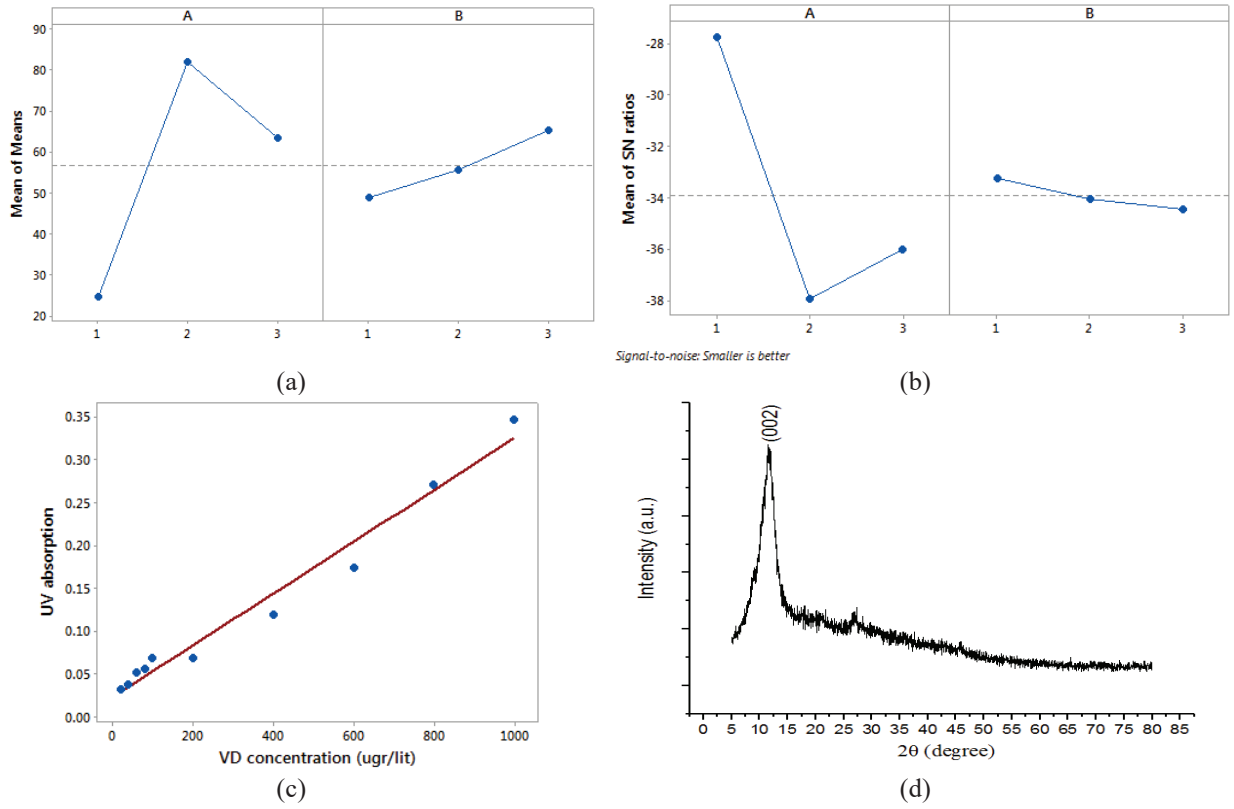

FIGURE 1. (a) Mean of means diagram, (b) Mean of signal-to-noise (SN) ratios, (c) VD standard curve prepared by Minitab software (version 17) and (d) nGO XRD pattern

Although, these results demonstrated that VD-loading had been greatly improved on the nGO nano-sheet in the presence of TW 80 as expected, the loading efficiency is still far away from being saturated. Therefore, a simple strategy to use the nGO-based nano-carrier cannot be enough.

Chemical Composition

The chemical structure and functional groups of synthesized nGO (GO), vitamin D (VD), and VD-loaded nGO (GOVD) were characterized by FTIR spectroscopy (fig. 2). Nicolet FTIR software (Omnic version 6.0) was used to analyze the spectra. As it can be seen in all the samples, the broad peak in the range of 3650-3200 cm^{-1} often gives clues to identifying the OH group. In this context, one of the reasons is rotational coupling, which may lead to a considerable amount of unresolved fine structure. In the GO spectrum, the peak at ~1600 cm^{-1} can be attributed to impurity or structural defects of graphite layers. However, a weak absorption near 1625 cm^{-1} can be due to the aromatic

C=C of the graphite layer. The characteristic peaks at 3448, 1738, and 1420 cm^{-1} are assigned to OH, C=O, and COOH, respectively [30]. These findings confirm the XRD results that the synthesized material is high-oxidized nGO.

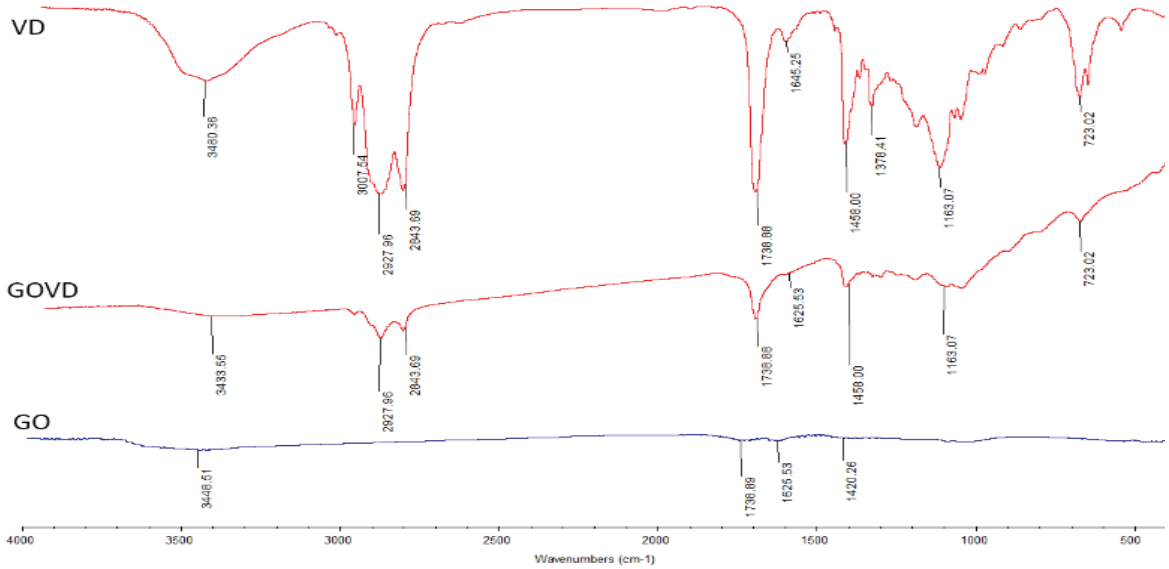

FIGURE 2. FTIR spectra of vitamin D_3 (VD), vitamin D_3-loaded graphene oxide (GOVD), and graphene oxide (GO)

The middle spectrum shows the original VD bands. The absorption bands at 2927 and 2843 cm^{-1} represent the symmetric stretching vibration and an asymmetric stretching of the methyl group, respectively. Therefore, they can be due to the presence of methyl groups in the VD structure. According to researchers, the peak at 1378 cm^{-1} is assigned to C-H bending motions, and this is while the C-H stretching appears at higher frequency (~3000 cm^{-1}) and overlaps with OH bands. Thus, further analysis will be needed to distinguish C-H bending from stretching. The spectrum exhibits one strongly absorbing peak at 1738 cm^{-1} which may correspond to the carbonyl group (C=O); but there is no carbonyl group in VD. Thus, it seems that the hydrogen bond of the hydroxyl group might be in resonance with the neighbor carbon. However, further analysis will still be needed to confirm this observation. A weak absorption near 1645 cm^{-1} confirmed the presence of C=C in the VD structure. The simple absorption, with few bands at about 720 cm^{-1} (723 cm^{-1}) usually shows bending (rocking) motion of CH_2 which is called the *long-chain band* [33].

TABLE 2. Assignment of spectra of VD and GO shown in Fig. 2.

Specimen	FTIR absorption band (cm^{-1})	Statement [a]	Specimen	FTIR absorption band (cm^{-1})	Statement [a]
VD	3480	O-H	GO	3448	O-H
	3007	S (C-H)		1738	C=O
	2927	V (CH_3)		1625	C=C
	2843	V_a (CH_3)		1420	COOH
	1738	C=O			
	1645	C=C			
	1378	B (C-H)			
	723	R (CH_2)			

[a] R (rocking vibration), B(bending vibration), S(stretching vibration), V (symemetric stretching vibration), V_a (asymmetric stertching vibration)

Additionally, we used FTIR spectroscopy to study the possible chemical interaction between GO and VD (GOVD). As expected, all the VD and GO spectra were detected in the GOVD spectrum. Briefly, most of the bands such as 3433, 2927, 2843, 1738, 1625, 1458, 1163, and 723 cm^{-1} were observed in the GOVD spectrum with somewhat smaller intensities and slight shifts. The combination of VD with GO resulted in shifts of the 3480 cm^{-1} band to 3433 cm^{-1}. These observations confirm the loading of VD on nGO-sheets. The FTIR absorption bands derived from Fig. 2 are given in Table 2.

CONCLUSION

A novel drug carrier for vitamin D delivery was prepared using a simple method. After preparation of graphene oxide according to the modified hummer's method, the drug was loaded in two different ways. It has been observed that using TW 80 had a marked effect on the drug loading percentage. In order to evaluate drug content, UV-Vis spectroscopy was employed to prepare the calibration curve. In this way, it has been observed that the VD:GO ratio plays the main role in the drug loading percentage, such that at 1:1 VD:GO ratio, the loading percentage reaches its highest value (75.37% ± 4.12). The FTIR results showed that there is no negative interaction between GO and VD, as well as protection of VD functional groups. This is attributed to the presence of GO that interacts with VD via π-π interaction and subsequent physical binding of VD. Moreover, TW 80 promotes this interaction to high drug loading. These results suggest that GO can be a promising vitamin D carrier for enhanced drug bioavailability in biomedical applications, especially in bone tissue engineering.

ACKNOWLEDGMENT

We wish to thank Ms. Masoomeh Haghbin-Nazarpak (Assistant Professor of Faculty of Biomedical Engineering, Amirkabir University of Technology (Tehran Polytechnic), 424 Hafez Ave, Tehran, Iran.) for her generous financial support.

REFERENCES

1. Torkaman, M., et al., *Comparison of the Vitamin D Status of Children Younger and Older Than 2 Years in Tehran: Are Supplements Really Necessary?* International Journal of Endocrinology and Metabolism, 2016(In press).
2. Hsiao, W.-C., et al., *Vitamin D3-inducible mesenchymal stem cell-based delivery of conditionally replicating adenoviruses effectively targets renal cell carcinoma and inhibits tumor growth.* Molecular pharmaceutics, 2012. **9**(5): p. 1396-1408.
3. Christakos, S., et al., *Vitamin D: Metabolism, Molecular Mechanism of Action, and Pleiotropic Effects.* Physiological reviews, 2016. **96**(1): p. 365-408.
4. Larriba, M.J., A.G. de Herreros, and A. Muñoz, *Vitamin D and the Epithelial to Mesenchymal Transition.* Stem Cells International, 2016.
5. St-Arnaud, R., *The direct role of vitamin D on bone homeostasis.* Archives of Biochemistry and Biophysics, 2008. **473**(2): p. 225-230.
6. Raulio, S., et al., *Successful nutrition policy: improvement of vitamin D intake and status in Finnish adults over the last decade.* The European Journal of Public Health, 2016: p. ckw154.
7. Im, N.K., et al., *Lupeol Isolated from Sorbus commixta Suppresses 1α, 25-(OH) 2D3-Mediated Osteoclast Differentiation and Bone Loss in Vitro and in Vivo.* Journal of Natural Products, 2016.
8. Artuso, A., et al., *Longitudinal Evaluation of Bone Mineral Density and Bone Metabolism Markers in Patients with Indolent Systemic Mastocytosis Without Osteoporosis*. Calcified Tissue International, 2016: p. 1-7.
9. Satué, M., et al., *Titanium implants coated with UV- irradiated vitamin D precursor and vitamin E: in vivo performance and coating stability.* Clinical Oral Implants Research, 2016.
10. Walia, N., et al., *Fish oil based vitamin D nanoencapsulation by ultrasonication and bioaccessibility analysis in simulated gastro-intestinal tract.* Ultrasonics Sonochemistry, 2017. **39**: p. 623-635.
11. Lin, Y., et al., *Corn protein hydrolysate as a novel nano-vehicle: Enhanced physicochemical stability and in vitro bioaccessibility of vitamin D3.* LWT - Food Science and Technology, 2016. **72**: p. 510-517.
12. Paucar, O.C., et al., *Production by spray chilling and characterization of solid lipid microparticles loaded with vitamin D3.* Food and Bioproducts Processing, 2016. **100, Part A**: p. 344-350.
13. Park, S.J., et al., *Development of nanostructured lipid carriers for the encapsulation and controlled release of vitamin D3.* Food Chemistry, 2017. **225**: p. 213-219.
14. Pedersen, J.N., et al., *Using protein-fatty acid complexes to improve vitamin D stability.* Journal of Dairy Science, 2016. **99**(10): p. 7755-7767.
15. Hans, M.L. and A.M. Lowman, *Biodegradable nanoparticles for drug delivery and targeting.* Current Opinion in Solid State and Materials Science, 2002. **6**(4): p. 319-327.

16. Sanchez, V.C., et al., *Biological interactions of graphene-family nanomaterials: an interdisciplinary review.* Chemical research in toxicology, 2011. **25**(1): p. 15-34.
17. Yang, K., et al., *Graphene in mice: ultrahigh in vivo tumor uptake and efficient photothermal therapy.* Nano letters, 2010. **10**(9): p. 3318-3323.
18. Nair, R., et al., *Unimpeded permeation of water through helium-leak–tight graphene-based membranes.* Science, 2012. **335**(6067): p. 442-444.
19. Novoselov, K.S., et al., *A roadmap for graphene.* Nature, 2012. **490**(7419): p. 192-200.
20. Liu, J., L. Cui, and D. Losic, *Graphene and graphene oxide as new nanocarriers for drug delivery applications.* Acta Biomaterialia, 2013. **9**(12): p. 9243-9257.
21. Feng, L. and Z. Liu, *Graphene in biomedicine: opportunities and challenges.* Nanomedicine, 2011. **6**(2): p. 317-324.
22. Sun, X., et al., *Nano-graphene oxide for cellular imaging and drug delivery.* Nano research, 2008. **1**(3): p. 203-212.
23. Barahuie, F., et al., *Graphene oxide as a nanocarrier for controlled release and targeted delivery of an anticancer active agent, chlorogenic acid.* Materials Science and Engineering: C, 2017. **74**: p. 177-185.
24. Lei, H., et al., *Adsorption of double-stranded DNA to graphene oxide preventing enzymatic digestion.* Nanoscale, 2011. **3**(9): p. 3888-3892.
25. Zhang, Q., et al., *NMR method for accurate quantification of polysorbate 80 copolymer composition.* Analytical chemistry, 2015. **87**(19): p. 9810-9816.
26. Prieto, C. and L. Calvo, *Performance of the biocompatible surfactant Tween 80, for the formation of microemulsions suitable for new pharmaceutical processing.* Journal of Applied Chemistry, 2013. **2013**.
27. Azhari, H., et al., *Stabilising cubosomes with Tween 80 as a step towards targeting lipid nanocarriers to the blood–brain barrier.* European Journal of Pharmaceutics and Biopharmaceutics, 2016. **104**: p. 148-155.
28. Yusuf, M., et al., *Polysorbate-80-coated, polymeric curcumin nanoparticles for in vivo anti-depressant activity across BBB and envisaged biomolecular mechanism of action through a proposed pharmacophore model.* Journal of microencapsulation, 2016. **33**(7): p. 646-655.
29. Hummers Jr, W.S. and R.E. Offeman, *Preparation of graphitic oxide.* Journal of the American Chemical Society, 1958. **80**(6): p. 1339-1339.
30. Imani, R., S.H. Emami, and S. Faghihi, *Nano-graphene oxide carboxylation for efficient bioconjugation applications: a quantitative optimization approach.* Journal of Nanoparticle Research, 2015. **17**(2): p. 1.
31. Depan, D., J. Shah, and R.D.K. Misra, *Controlled release of drug from folate-decorated and graphene mediated drug delivery system: Synthesis, loading efficiency, and drug release response.* Materials Science and Engineering: C, 2011. **31**(7): p. 1305-1312.
32. Li, Y., L. Tang, and J. Li, *Preparation and electrochemical performance for methanol oxidation of Pt/graphene nanocomposites.* Electrochemistry Communications, 2009. **11**(4): p. 846-849.
33. Pavia, D.L., et al., *Introduction to spectroscopy*. 2008: Cengage Learning.